Proceedings of ALGORITMY 2005
pp. 32–41

TANGENTIALLY STABILIZED LAGRANGIAN ALGORITHM FOR ELASTIC CURVE EVOLUTION DRIVEN BY INTRINSIC LAPLACIAN OF CURVATURE

KAROL MIKULA * AND DANIEL ŠEVČOVIČ †

Abstract. We suggest a stable Lagrangian method for computing elastic curve evolution driven by the intrinsic Laplacian of curvature (called also surface diffusion of curves). The algorithm for solving such a geometric evolution is based on a numerical solution to a fourth order intrinsic diffusion equation. The stability of the method is enhanced on by asymptotically uniform grid point tangential redistribution, preventing formation of various instabilities as merging of grid points and/or formation of swallow-tails. The stabilized method not only allows for larger time steps without loosing stability but also more accurately preserves the area encompassed by flowing curves which is a basic analytical property of a surface diffusion flow.

Key words. elastic curves, surface diffusion, numerical solution, semi-implicit scheme, tangential redistribution

AMS subject classifications.

1. Introduction. In this paper we suggest a method for computing evolution of closed smooth plane curves Γ_t, $t \geq 0$, driven by the normal velocity β which is a function of the intrinsic Laplacian (i.e., the second derivative with respect to the arclength parameter s) of its curvature k, namely

$$\beta = -\partial_s^2 k \,. \tag{1.1}$$

Since for the area A_t of a closed smooth evolving curve Γ_t we have $\frac{dA_t}{dt} + \int_{\Gamma_t} \beta ds = 0$ and $\int_{\Gamma_t} \partial_s^2 k \, ds = 0$, Eq. (1.1) conserves the area enclosed by a moving elastic curve, see e.g. also [7]. In three dimensions an analogy of (1.1), fulfilling the volume conservation property of evolving 2D surfaces, is called the surface diffusion. The motion of elastic curves, e.g. the model of Euler-Bernoulli elastic rod, is an important problem in structural mechanics. The elastic curve evolution and surface diffusion can be also found in many further practical problems as sintering (in brick production), formation of rock strata from sandy sediments, metal thin film growth and motions in microfabrication of electronic components, interface motions in crystal growth, or in new applications like image segmentation and computer and human vision modeling (see e.g. [18, 3, 9, 4, 19, 17]).

In this paper, we present a solution of (1.1) by the so-called direct or Lagrangian approach. The main idea of the Lagrangian approach is to represent a flow of planar curves by the position vector x which is a solution to the geometric equation $\partial_t x = \beta\vec{N} + \alpha\vec{T}$ where $\vec{N}, \vec{T}$ are the unit inward normal and tangent vectors. The presence of a tangential velocity α in the position vector equation has no impact on the shape of evolving curves. Therefore a natural setting $\alpha = 0$ has been chosen for analytical as well as numerical treatment (see e.g. [1, 6, 16, 11, 12, 13] in the case of linear and nonlinear curvature driven evolutions, or [7, 2] in case of elastic flows and surface diffusion). However, as it was shown in [14, 15] for general (nonlinear, anisotropic, with external forces) curvature driven motions (see also [8, 10])

*Department of Mathematics, Slovak University of Technology, Radlinského 11, 813 68 Bratislava, Slovak Republic (mikula@vox.svf.stuba.sk).
†Inst. of Applied Mathematics, Faculty of Mathematics, Physics & Informatics, Comenius University, 842 48 Bratislava, Slovak Republic (sevcovic@fmph.uniba.sk).

This work was supported by VEGA grants 1/0313/03 and 1/7677/20.

and, as it will be shown here for the case of elastic curve flows, incorporation of a suitable tangential velocity into governing equations stabilizes numerical computations significantly. It prevents the Lagrangian algorithm from its main drawbacks, the merging of numerical grid points and also allows for large time steps without loosing stability.

The outline of the paper is as follows. In section 2 we present a closed governing system of equations for the curvature, tangential angle, local length and position vector describing evolution of plane curves satisfying (1.1). These equations contain a free parameter - the tangential velocity α. In section 3 we present suitable strategies how to choose α guaranteeing, e.g., an asymptotically uniform redistribution of grid points along an evolved curve. In section 4 our numerical scheme for full space time discretization is presented. The governing system of PDEs contains fourth and second order intrinsic differential terms as well as the first order advection and strong reaction terms. These nonlinear equations are discretized in time using semi-implicit scheme, so finally we end up with pentadiagonal linear systems in every time step. Interestingly, utilizing tangential redistribution, such systems can be solved in a fast way by simple Gauss-Seidel iterations. In [7] a semi-implicit scheme was combined with a splitting of the fourth order position vector equation into two second order problems and then linear finite element method was applied. The redistribution was used only as a postprocessing step. Here we incorporate suitable tangential redistribution into the governing system of equations and then we apply intrinsic finite differences (the so-called flowing finite volumes directly to the fourth order equations). Results of our numerical approximations are discussed in section 5.

2. Governing equations. An embedded regular plane curve Γ can be parameterized by a smooth function $x : S^1 \to \mathbb{R}^2$, i.e. $\Gamma = \text{Image}(x) := \{x(u), u \in S^1\}$, for which $g = |\partial_u x| > 0$. Taking into account the periodic boundary conditions at $u = 0, 1$ we shall hereafter identify S^1 with the interval $[0, 1]$. The unit arc-length parameterization will be denoted by s, so $ds = g\,du$. The tangent vector $\vec{T}$ and the signed curvature k of Γ satisfy $\vec{T} = \partial_s x = \partial_u x/g$, $k = \partial_s x \wedge \partial_s^2 x = \partial_u x \wedge \partial_u^2 x/g^3$. Moreover, we choose the unit inward normal vector $\vec{N}$ such that $\vec{T} \wedge \vec{N} = 1$ where $\vec{a} \wedge \vec{b}$ is the determinant of the 2×2 matrix with column vectors $\vec{a}, \vec{b}$. By ν we denote the tangent angle to Γ, i.e. $\vec{T} = (\cos\nu, \sin\nu)^T$ and, by Frenét's formulae, $\partial_s \vec{T} = k\vec{N}$, $\partial_s \vec{N} = -k\vec{T}$ and $\partial_s \nu = k$.

Let a regular smooth initial curve $\Gamma_0 = \text{Image}(x_0)$ be given. A family of plane curves $\Gamma_t = \text{Image}(x(.,t)), t \in [0, T)$, satisfying (1.1) can be represented by a solution to the following system of PDEs

$$\partial_t k = \partial_s^2 \beta + \alpha \partial_s k + k^2 \beta\,, \tag{2.1}$$

$$\partial_t \nu = \partial_s \beta + \alpha k\,, \tag{2.2}$$

$$\partial_t g = -gk\beta + g\partial_s \alpha\,, \tag{2.3}$$

$$\partial_t x = \beta \vec{N} + \alpha \vec{T} \tag{2.4}$$

subject to initial conditions $k(.,0) = k_0\,,\ \nu(.,0) = \nu_0\,,\ g(.,0) = g_0\,,\ x(.,0) = x_0(.)$ and periodic boundary conditions at $u = 0, 1$ except of ν for which we require the boundary condition $\nu(1,t) = \nu(0,t) + 2\pi$ (cf. [14]).

3. Suitable choices of the tangential velocity. Notice that the functional α is still undetermined and it may depend on other variables in various ways including local or nonlocal dependences. The idea behind construction of a suitable tangential velocity functional α is rather simple and consists in the analysis of the quantity $\theta = \ln(g/L)$ which can be viewed as the logarithm of the relative local length g/L.

If we denote by L_t the length of a curve Γ_t, i.e. $L_t = \int_{\Gamma_t} ds = \int_0^1 g(u,t)\, du$, then by taking into account periodicity of α and equation (2.3) we conclude

$$\frac{d}{dt} L_t + \langle k\beta \rangle_{\Gamma_t} L_t = 0, \tag{3.1}$$

where $\langle k\beta\rangle_\Gamma = \frac{1}{L}\int_\Gamma k\beta\, ds$ denotes a nonlocal quantity, the average of $k\beta$ over the curve Γ. Hence it follows from (2.3) and (3.1) that

$$\partial_t \theta + k\beta - \langle k\beta\rangle_\Gamma = \partial_s \alpha\,. \tag{3.2}$$

By a suitable choice of $\partial_s\alpha$ in the right hand side of (3.2) appropriately we can therefore control behavior of θ.

A general (nonlocal) choice of α is based on the following setup:

$$\partial_s \alpha = k\beta - \langle k\beta\rangle_\Gamma + \left(e^{-\theta} - 1\right)\omega(t) \tag{3.3}$$

where $\omega \in L^1_{loc}([0, T_{max}))$ and T_{max} is a maximal existence time of evolving curve. Notice that α can be uniquely computed from (3.3) under an additional constraint, e.g., $\alpha(0,t) = 0$. The choice $\omega(t) \equiv 0$ yields $\partial_t\theta = 0$ in (3.2) and consequently,

$$\frac{g(u,t)}{L_t} = \frac{g(u,0)}{L_0} \quad \text{for any } u \in S^1,\ t \in [0, T_{max})\,,$$

so we obtain a tangential *redistribution preserving relative local length* [8, 14]. If we suppose

$$\int_0^{T_{max}} \omega(\tau)\, d\tau = +\infty \tag{3.4}$$

then, after insertion of (3.3) into (3.2) and solving the corresponding ODE $\partial_t\theta = \left(e^{-\theta} - 1\right)\omega(t)$, we obtain $\theta(u,t) \to 0$ as $t \to T_{max}$ and hence

$$\frac{g(u,t)}{L_t} \to 1 \quad \text{as } t \to T_{max} \quad \text{uniformly w.r. to } u \in S^1.$$

In this case redistribution of grid points along a curve becomes uniform as t approaches the maximal time of existence T_{max} and we call it *asymptotically uniform (AU) redistribution*. On the other hand, if apriori know that $T_{max} = +\infty$ (as it is the case of (1.1) with a Jordan simple initial curve) one can choose $\omega(t) = \kappa_1$, where $\kappa_1 > 0$ is a positive constant in order to meet the assumption (3.4). Summarizing, a suitable general (nonlocal) choice of the tangential velocity functional α is given by a solution to

$$\partial_s\alpha = k\beta - \langle k\beta\rangle_\Gamma + (L/g - 1)\,\omega,\ \ \omega = \kappa_1 + \kappa_2\langle k\beta\rangle_\Gamma,\ \ \alpha(0,t) = 0\,, \tag{3.5}$$

where $\kappa_1, \kappa_2 \geq 0$ are given constants. If we insert tangential velocity functional α computed from (3.5) into (2.1)–(2.4) and make use of the identity $\alpha\partial_s k = \partial_s(\alpha k) - k\partial_s\alpha$ then the curvature and local length equations can be rewritten as follows:

$$\partial_t k = \partial_s^2\beta + \partial_s(\alpha k) + k\langle k\beta\rangle_\Gamma + (1 - L/g)\, k\omega\,, \tag{3.6}$$

$$\partial_t g = -g\langle k\beta\rangle_\Gamma + (L - g)\omega\,, \tag{3.7}$$

We can see that the "pointwise" influence of the term $k^2\beta$ in (2.1) and (2.3) has been replaced by the "averaged" term $k\langle k\beta\rangle_\Gamma$ in (3.6) and (3.7). It enables us to construct an efficient and stable numerical scheme discussed in next section.

Another possibility for grid points redistribution along evolved curves is based on a tangential velocity functional defined locally. If we take $\alpha = \partial_s\theta = \partial_s \ln(g/L) = \partial_s \ln g$ (see also [5]), i.e. $\partial_s\alpha = \partial_s^2\theta$ then the constitutive equation (3.2) reads as follows: $\partial_t\theta + k\beta - \langle k\beta\rangle_\Gamma = \partial_s^2\theta$. Since this equation has a parabolic nature one can expect that θ will be redistributed along the curve Γ due to the diffusion process and we call it *locally diffusive (LD) redistribution*. Indeed, by inserting $\alpha = \partial_s(\ln g)$ into (2.3) we obtain $\partial_t g = -gk\beta + g\partial_s^2(\ln g)$, which is a nonlinear parabolic equation for g.

4. Numerical scheme. In our numerical solution we consider tangential velocity given by a linear combination of nonlocal and local tangential redistributions discussed in the previous section. Let us denote $\eta = \ln g$. Then we have $\theta = \ln(g/L) = \eta - \ln L$, and, for the redistribution functional α, we obtain

$$\partial_s\alpha = \varepsilon_1(k\beta - \langle k\beta\rangle_\Gamma) + \omega\,(L/g - 1) + \varepsilon_2\partial_s^2\eta \tag{4.1}$$

where $\varepsilon_1, \omega, \varepsilon_2$ are weights for redistribution preserving relative local length, asymptotically uniform redistribution and locally diffusive redistribution, respectively. Since

$$\begin{aligned}\partial_s^4 x &= \partial_s^3\vec{T} = \partial_s^2(k\vec{N}) = \partial_s^2 k\vec{N} + 2\partial_s k\partial_s\vec{N} + k\partial_s^2\vec{N} = \partial_s^2 k\vec{N} - 2(\partial_s k)k\vec{T} - k\partial_s(k\vec{T})\\ &= \partial_s^2 k\vec{N} - 3k(\partial_s k)\vec{T} - k^2\partial_s\vec{T} = \partial_s^2 k\vec{N} - \frac{3}{2}\partial_s(k^2)\partial_s x - k^2\partial_s^2 x,\end{aligned}$$

we have $-\partial_s^2 k\vec{N} = -\partial_s^4 x - k^2\partial_s^2 x - \frac{3}{2}\partial_s(k^2)\partial_s x$. Moreover, as $k = \partial_s\nu$ we have $\partial_s\beta = -\partial_s^4\nu$. Thus the governing system of equations (2.1)–(2.4) for the elastic flow (1.1) with tangential redistribution can be written as follows:

$$\partial_t k = -\partial_s^4 k + \partial_s(\alpha k) + k(k\beta - \partial_s\alpha), \tag{4.2}$$

$$\partial_t\nu = -\partial_s^4\nu + \alpha\partial_s\nu, \tag{4.3}$$

$$\partial_t\eta = -k\beta + \partial_s\alpha, \quad g = \exp(\eta), \tag{4.4}$$

$$\partial_t x = -\partial_s^4 x - k^2\partial_s^2 x + \left(\alpha - \frac{3}{2}\partial_s(k^2)\right)\partial_s x\,. \tag{4.5}$$

In our computational method a numerically evolved curve is represented by discrete plane points x_i^j where the index $i = 1, ..., n,$ denotes space discretization and the index $j = 0, ..., m,$ denotes a discrete time stepping. The linear approximation of an evolving curve in j-th discrete time step is thus given by a polygon with vertices $x_i^j, i = 1, ..., n.$ Due to periodicity conditions we will use also additional values $x_{-1}^j = x_{n-1}^j$, $x_0^j = x_n^j$, $x_{n+1}^j = x_1^j$, $x_{n+2}^j = x_2^j$. If we take a uniform division of the time interval $[0, T]$ with a time step $\tau = \frac{T}{m}$ and a uniform division of the fixed parameterization interval $[0, 1]$ with a step $h = \frac{1}{n}$, a point x_i^j corresponds to $x(ih, j\tau)$. The systems of difference equations corresponding to (4.1) – (4.5) will be given for discrete quantities α_i^j, η_i^j, r_i^j, k_i^j, ν_i^j, x_i^j, $i = 1, ..., n,\ j = 1, ..., m,$ representing approximations of the unknowns α, η, gh, k, ν, and x, respectively. Here α_i^j represents tangential velocity of a flowing node x_i^j, and $\eta_i^j, r_i^j \approx |x_i^j - x_{i-1}^j|$, k_i^j, ν_i^j represent piecewise constant approximations of the corresponding quantities in the so-called *flowing finite volume* $\left[x_{i-1}^j, x_i^j\right]$. We will also use the corresponding flowing dual volumes $\left[\tilde{x}_{i-1}^j, \tilde{x}_i^j\right]$, where $\tilde{x}_i^j = \frac{x_{i-1}^j + x_i^j}{2}$, with approximate lengths $q_i^j \approx |\tilde{x}_i^j - \tilde{x}_{i-1}^j|$. At the j-th discrete time step, we first find discrete values of the tangential velocity α_i^j by discretization of (4.1). Then the values of redistribution parameter η_i^j are computed and utilized for updating discrete local lengths r_i^j by discretizing equations (4.4). Using already computed local lengths, the intrinsic derivatives are approximated in (4.2), (4.3) and (4.5), and pentadiagonal systems with periodic boundary conditions are constructed and solved for discrete curvatures k_i^j, tangent angles ν_i^j and position vectors x_i^j. In the sequel, we present in detail our discretization.

Using r_i^{j-1} as an approximation of the length of the flowing finite volume $\left[x_{i-1}^{j-1}, x_i^{j-1}\right]$ at the previous time step we construct difference approximation of the intrinsic derivative $\partial_s \alpha \approx \frac{\alpha_i^j - \alpha_{i-1}^j}{r_i^{j-1}}$ and taking all further quantities in (4.1) from the previous time step we obtain the following expression for *discrete values of the tangential velocity:*

$$\alpha_i^j = \alpha_{i-1}^j + \varepsilon_1 \left(r_i^{j-1} k_i^{j-1} \beta_i^{j-1} - r_i^{j-1} B^{j-1}\right) + \omega(M^{j-1} - r_i^{j-1}) + \varepsilon_2 \left(\frac{\eta_{i+1}^{j-1} - \eta_i^{j-1}}{q_i^{j-1}} - \frac{\eta_i^{j-1} - \eta_{i-1}^{j-1}}{q_{i-1}^{j-1}} \right),$$

where

$$q_i^j = \frac{r_i^j + r_{i+1}^j}{2}, \ \ \beta_i^j = -\frac{1}{r_i^j} \left(\frac{k_{i+1}^j - k_i^j}{q_i^j} - \frac{k_i^j - k_{i-1}^j}{q_{i-1}^j} \right), \ i = 1, ..., n,$$

$$M^{j-1} = \frac{1}{n} L^{j-1}, \ \ L^{j-1} = \sum_{l=1}^{n} r_l^{j-1}, \ B^{j-1} = \frac{1}{L^{j-1}} \sum_{l=1}^{n} r_l^{j-1} k_l^{j-1} \beta_l^{j-1},$$

$\omega = \kappa_1 + \kappa_2 B^{j-1}$, and $\alpha_0^j = 0$, i.e. the point x_0^j is moved in the normal direction. Then, a similar strategy for discretization of (4.4) gives us

$$r_i^{j-1} \frac{\eta_i^j - \eta_i^{j-1}}{\tau} = (\varepsilon_1 - 1) r_i^{j-1} k_i^{j-1} \beta_i^{j-1} - \varepsilon_1 r_i^{j-1} B^{j-1} + \omega(M^{j-1} - r_i^{j-1}) + \varepsilon_2 \left(\frac{\eta_{i+1}^j - \eta_i^j}{q_i^{j-1}} - \frac{\eta_i^j - \eta_{i-1}^j}{q_{i-1}^{j-1}} \right),$$

for $i = 1, ..., n, \ \ \eta_0^j = \eta_n^j, \ \ \eta_{n+1}^j = \eta_1^j$. Note that this is either an updating formula in the case $\varepsilon_2 = 0$ or a tridiagonal system (if $\varepsilon_2 \neq 0$) for *new values of a redistribution parameter* η. Next we *update local lengths* by the rule:

$$r_i^j = \exp(\eta_i^j), \ \ i = 1, ..., n, \ \ r_{-1}^j = r_{n-1}^j, \ \ r_0^j = r_n^j, \ \ r_{n+1}^j = r_1^j, \ \ r_{n+2}^j = r_2^j.$$

Subsequently, new local lengths are used for approximation of intrinsic derivatives in (4.2), (4.3), and (4.5). First, we derive a discrete analogy of the curvature equation (4.2). We have to approximate the 4-th order derivative of curvature inside the flowing finite volume $[x_{i-1}, x_i]$, $i = 1, ..., n$ (for a moment we omit upper index j). For that goal we take

$$\partial_s^4 k(\tilde{x}_i) \approx \frac{\partial_s^3 k(x_i) - \partial_s^3 k(x_{i-1})}{r_i} \approx \frac{1}{r_i} \left(\frac{\partial_s^2 k(\tilde{x}_{i+1}) - \partial_s^2 k(\tilde{x}_i)}{q_i} - \frac{\partial_s^2 k(\tilde{x}_i) - \partial_s^2 k(\tilde{x}_{i-1})}{q_{i-1}} \right)$$
$$\approx \frac{1}{r_i q_i r_{i+1} q_{i+1}} k_{i+2} - \left(\frac{1}{r_i q_i r_{i+1} q_{i+1}} + \frac{1}{r_i q_i^2 r_{i+1}} + \frac{1}{r_i^2 q_i^2} + \frac{1}{r_i^2 q_i q_{i-1}} \right) k_{i+1} +$$
$$\left(\frac{1}{r_i q_i^2 r_{i+1}} + \frac{1}{r_i^2 q_i^2} + \frac{2}{r_i^2 q_i q_{i-1}} + \frac{1}{r_i^2 q_{i-1}^2} + \frac{1}{r_i q_{i-1}^2 r_{i-1}} \right) k_i +$$
$$\left(\frac{1}{r_i^2 q_i q_{i-1}} + \frac{1}{r_i^2 q_{i-1}^2} + \frac{1}{r_i q_{i-1}^2 r_{i-1}} + \frac{1}{r_i q_{i-1} r_{i-1} q_{i-2}} \right) k_{i-1} + \frac{1}{r_i q_{i-1} r_{i-1} q_{i-2}} k_{i-2}.$$

Approximating first order terms in (4.2) by central differences and taking semi-implicit time stepping we obtain following *pentadiagonal system* with periodic boundary conditions for *new discrete values of curvature*:

$$a_i^j k_{i-2}^j + b_i^j k_{i-1}^j + c_i^j k_i^j + d_i^j k_{i+1}^j + e_i^j k_{i+2}^j = f_i^j, \ \ i = 1, ..., n,$$

subject to periodic b.c. $k_{-1}^j = k_{n-1}^j, \ \ k_0^j = k_n^j, \ \ k_{n+1}^j = k_1^j, \ \ k_{n+2}^j = k_2^j$, where

$$a_i^j = \frac{1}{q_{i-1}^j r_{i-1}^j q_{i-2}^j}, \ \ e_i^j = \frac{1}{q_i^j r_{i+1}^j q_{i+1}^j}, \ \ f_i^j = \frac{r_i^j}{\tau} k_i^{j-1},$$

$$b_i^j = -\left(\frac{1}{r_i^j q_i^j q_{i-1}^j} + \frac{1}{r_i^j (q_{i-1}^j)^2} + \frac{1}{(q_{i-1}^j)^2 r_{i-1}^j} + \frac{1}{q_{i-1}^j r_{i-1}^j q_{i-2}^j} \right) + \frac{\alpha_{i-1}^j}{2}$$

$$d_i^j = -\left(\frac{1}{q_i^j r_{i+1}^j q_{i+1}^j} + \frac{1}{(q_i^j)^2 r_{i+1}^j} + \frac{1}{r_i^j (q_i^j)^2} + \frac{1}{r_i^j q_i^j q_{i-1}^j} \right) - \frac{\alpha_i^j}{2}$$

$$c_i^j = \frac{1}{(q_i^j)^2 r_{i+1}^j} + \frac{1}{r_i^j (q_i^j)^2} + \frac{2}{r_i^j q_i^j q_{i-1}^j} + \frac{1}{r_i^j (q_{i-1}^j)^2} + \frac{1}{(q_{i-1}^j)^2 r_{i-1}^j} + \frac{r_i^j}{\tau} - r_i^{j-1} k_i^{j-1} \beta_i^{j-1} + \frac{\alpha_i^j}{2} - \frac{\alpha_{i-1}^j}{2}.$$

Using a similar approximation as above also for equation (4.3) we end up with following pentadiagonal system with 2π-shifted periodic boundary conditions for *new discrete values of the tangent angle:*

$$a_i^j \nu_{i-2}^j + b_i^j \nu_{i-1}^j + C_i^j \nu_i^j + d_i^j \nu_{i+1}^j + e_i^j \nu_{i+2}^j = F_i^j, \ \ i = 1, ..., n\,,$$

subject to mod 2π periodic b.c. $\nu_{-1}^j = \nu_{n-1}^j - 2\pi, \ \ \nu_0^j = \nu_n^j - 2\pi, \ \ \nu_{n+1}^j = \nu_1^j + 2\pi, \ \ \nu_{n+2}^j = \nu_2^j + 2\pi$ where $C_i^j = \frac{r_i^j}{\tau} - (a_i^j + b_i^j + d_i^j + e_i^j)$, and $F_i^j = \frac{r_i^j}{\tau} \nu_i^{j-1}$.

In order to construct discretization of equation (4.5) we approximate the intrinsic derivatives in a dual volume $[\tilde{x}_{i-1}, \tilde{x}_i]$. For approximation of 4-th order intrinsic derivative of the position vector we take similar approach as above for curvature, but in the middle point x_i of the dual volume. In such a way and using the semi-implicit approach, we end up with *two tridiagonal systems for updating the discrete position vector:*

$$\mathcal{A}_i^j x_{i-2}^j + \mathcal{B}_i^j x_{i-1}^j + \mathcal{C}_i^j x_i^j + \mathcal{D}_i^j x_{i+1}^j + \mathcal{E}_i^j x_{i+2}^j = \mathcal{F}_i^j \ , \ i = 1, ..., n\,,$$

subject to periodic b.c. $x_{-1}^j = x_{n-1}^j, \ \ x_0^j = x_n^j, \ \ x_{n+1}^j = x_1^j, \ \ x_{n+2}^j = x_2^j$ where

$$\mathcal{A}_i^j = \frac{1}{r_i^j q_{i-1}^j r_{i-1}^j}, \ \mathcal{C}_i^j = \frac{q_i^j}{\tau} - (\mathcal{A}_i^j + \mathcal{B}_i^j + \mathcal{D}_i^j + \mathcal{E}_i^j), \ \mathcal{E}_i^j = \frac{1}{r_{i+1}^j q_{i+1}^j r_{i+2}^j}, \ \mathcal{F}_i^j = \frac{q_i^j}{\tau} x_i^{j-1},$$

$$\mathcal{B}_i^j = -\left(\frac{1}{r_i^j q_{i-1}^j r_{i-1}^j} + \frac{1}{(r_i^j)^2 q_{i-1}^j} + \frac{1}{(r_i^j)^2 q_i^j} + \frac{1}{r_i^j q_i^j r_{i+1}^j} \right) + \frac{(k_{i+1}^j)^2 + (k_i^j)^2}{2 r_i^j} + \frac{\alpha_i^j}{2} - \frac{3}{2} \frac{(k_{i+1}^j)^2 - (k_i^j)^2}{q_i^j}$$

$$\mathcal{D}_i^j = -\left(\frac{1}{r_i^j q_i^j r_{i+1}^j} + \frac{1}{(r_{i+1}^j)^2 q_i^j} + \frac{1}{(r_{i+1}^j)^2 q_{i+1}^j} + \frac{1}{r_{i+1}^j q_{i+1}^j r_{i+2}^j} \right) + \frac{(k_{i+1}^j)^2 + (k_i^j)^2}{2 r_{i+1}^j} - \frac{\alpha_i^j}{2} + \frac{3}{2} \frac{(k_{i+1}^j)^2 - (k_i^j)^2}{q_i^j}.$$

TABLE 5.1
Values of several quantities in evolution of initial ellipse computed without tangential redistribution.

time	Length	Area	Isoperimetric ratio	$\min r_i$ / $\max r_i$
0	9.686855	6.279052	1.1892	0.50
0.2	9.163085	6.275085	1.0647	0.36
0.4	8.972153	6.272706	1.0212	0.27
0.6	8.907421	6.270957	1.0068	0.24
0.8	8.886850	6.269648	1.0024	0.23
1.0	8.880245	6.268606	1.0010	0.22
2.0	8.875194	6.264775	1.0005	0.21

TABLE 5.2
Several quantities in evolution of initial ellipse computed with AU redistribution ($\varepsilon_1 = 1$, $\kappa_1 = 2$, $\kappa_2 = 0$, $\varepsilon_2 = 0$).

time	Length	Area	Isoperimetric ratio	$\min r_i$ / $\max r_i$
0	9.686855	6.279052	1.1892	0.50
0.2	9.164443	6.278972	1.0644	0.63
0.4	8.974767	6.279188	1.0207	0.74
0.6	8.911797	6.279617	1.0064	0.82
0.8	8.892818	6.280140	1.0020	0.87
1.0	8.887552	6.280698	1.0008	0.92
2.0	8.887520	6.283582	1.0003	0.99

The initial quantities for the algorithm are computed from discrete representation of the initial curve x_0, for details see [15]. Every pentadiagonal system is solved by Gauss-Seidel iterations. We stop the iterations if a difference of subsequent Gauss-Seidel iterations in maximum norm is less than TOL $= 10^{-10}$.

5. Discussion on numerical experiments. First we compute numerically time evolution of the initial ellipse with halfaxes ratio 2:1 in time interval $[0, 2]$. The evolving curve is represented by $n = 100$ grid points and we use discrete time step $\tau = 0.001$. In Tables 5.1, 5.2 and 5.3 we present evolution of the length, area, isoperimetric ratio $L_t^2/(4\pi A_t)$ and the ratio of minimal and maximal grid point distances for different tangential redistribution strategies. In all cases the evolution of isoperimetric ratio to 1 indicates convergence of evolving curve to a circle. The evolution of $\min r_i/\max r_i$ in the case without tangential redistribution indicates accumulation of some curve representing grid points and a poor resolution in other parts of the asymptotical shape, see also Figure 5.1 left. In the case of asymptotically uniform (AU) tangential redistribution, we see convergence of this ratio to 1 and thus a uniform discrete resolution of the asymptotical shape, see Figure 5.1 right. Although obtained by different mechanism, a similar behavior is observed using locally diffusive (LD) redistribution. One can make also further important observation - the initial area is better conserved using tangential redistributions. For the same initial curve such phenomenon is studied in Table 5.4. Refining the curve resolution, and correspondingly the time step ($\tau \approx h^2$), we see that the errors in enclosed area converge to zero and an approximate second order experimental convergence rate with respect to h can be observed. However, the area errors are significantly lower in computations with tangential redistribution. Especially, using our asymptotically uniform redistribution (fourth column of Table 5.4, $\varepsilon_1 = 1$, $\kappa_1 = 1$, $\kappa_2 = 0$, $\varepsilon_2 = 0$) is superior, the area errors are more that 10 times lower than in computations without redistribution.

Next we present evolution of several nontrivial initial curves driven by (1.1). We show evolution of the highly nonconvex initial curve (Figure 5.2 top left) and the interesting dynamics of two evolving self-intersecting curves, the quatrefoil (Figure 5.3 top left) and the

TABLE 5.3

Values of several quantities in evolution of initial ellipse computed with LD redistribution ($\varepsilon_1 = 0$, $\omega = 0$, $\varepsilon_2 = 1$).

time	Length	Area	Isoperimetric ratio	$\min r_i \;/\; \max r_i$
0	9.686855	6.279052	1.1892	0.50
0.2	9.163794	6.276898	1.0646	0.51
0.4	8.973502	6.275995	1.0210	0.54
0.6	8.909531	6.275432	1.0065	0.60
0.8	8.889626	6.275057	1.0021	0.68
1.0	8.883579	6.274777	1.0008	0.75
2.0	8.880521	6.273700	1.0003	0.95

TABLE 5.4

Maximal errors in area enclosed by evolving curve starting with initial ellipse in time interval $[0, 0.96]$.

n	τ	No redistribution	AU redistribution	LD redistribution
10	0.064	0.352329	0.095360	0.088189
20	0.016	0.141946	0.012779	0.042644
40	0.004	0.045651	0.002907	0.016452
80	0.001	0.012214	0.000916	0.004930
160	0.00025	0.002296	0.000197	0.001067

Lissajous curve (Figure 5.4 top left). We use $n = 100$ grid points for discrete curve representations and asymptotically uniform redistribution with $\varepsilon_1 = 1$, $\kappa_1 = 1$, $\kappa_2 = 1$, $\varepsilon_2 = 0$. Since elastic curve dynamics is very fast in case of highly varying curvature along the curve, in the first experiment we have chosen time step $\tau = 10^{-6}$, and in the case of quatrefoil and Lissajous curve we use $\tau = 10^{-5}$. With such chosen time steps, the computations using tangential redistribution are stable and fast, few tens of Gauss-Seidel iterations are needed to arrive to convergent solution with our TOL in every time step. Without redistribution, e.g. in the case of nonconvex curve plotted in Figure 5.2, the computation is unstable with the same time step. The ratio $\min r_i / \max r_i$ degenerates soon and consequently the computations crash. In order to have stable numerical evolution we have to choose 10 times smaller time step $\tau = 10^{-7}$ and also in such case the convergence of iterations is much slower, thousands of them are necessary.

Acknowledgment. We thank to Prof. John W. Barrett for attracting our attention to application of the tangential redistribution to elastic curve evolution.

REFERENCES

[1] S. B. ANGENENT, M. E. GURTIN, *Multiphase thermomechanics with an interfacial structure 2. Evolution of an isothermal interface,* Arch. Rat. Mech. Anal., 108 (1989), pp. 323–391.

[2] E. BÄNSCH, P. MORIN, R. NOCHETTO, *Surface diffusion of graphs: Variational formulation, error analysis, and simulation,* SIAM J. Numer. Anal., 42 (2004), pp. 773–799.

[3] J. W. CAHN, J. E. TAYLOR, *Surface motion by surface diffusion,* Acta Metallica Materiala, 42 (1994), pp. 1045–1063.

[4] U. CLARENZ, U. DIEWALD, G. DZIUK, M. RUMPF, R. RUSU, *A finite element method for surface restoration with smooth boundary conditions,* Computer Aided Geometric Design, 21 (2004), pp. 427–445.

[5] K. DECKELNICK, *Weak solutions of the curve shortening flow,* Calc. Var. Partial Differ. Equ., 5 (1997), pp. 489–510.

[6] G. DZIUK, *Convergence of a semi discrete scheme for the curve shortening flow,* Mathematical Models and Methods in Applied Sciences, 4 (1994), pp. 589–606.

[7] G. DZIUK, E. KUWERT, R. SCHATZLE, *Evolution of elastic curves in $\mathbb{R}^n$: existence and computation,* SIAM J. Math. Anal., 33 (2002), pp. 1228–1245.

[8] T.Y. HOU, J. LOWENGRUB, M. SHELLEY, *Removing the stiffness from interfacial flows and surface tension,* J. Comput. Phys., 114 (1994), pp. 312–338.

[9] M. KASS, A. WITKIN, D. TERZOPULOS, *Snakes: active contour models,* International Journal of Computer

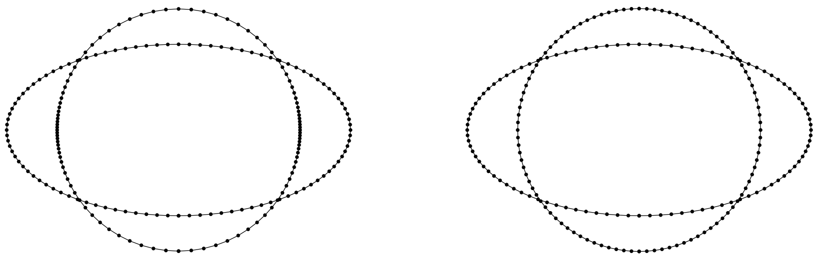

FIG. 5.1. *Initial ellipse and the representing gridpoints together with circular asymptotical shapes and their discrete representations without (left) and with (right) tangential redistributions.*

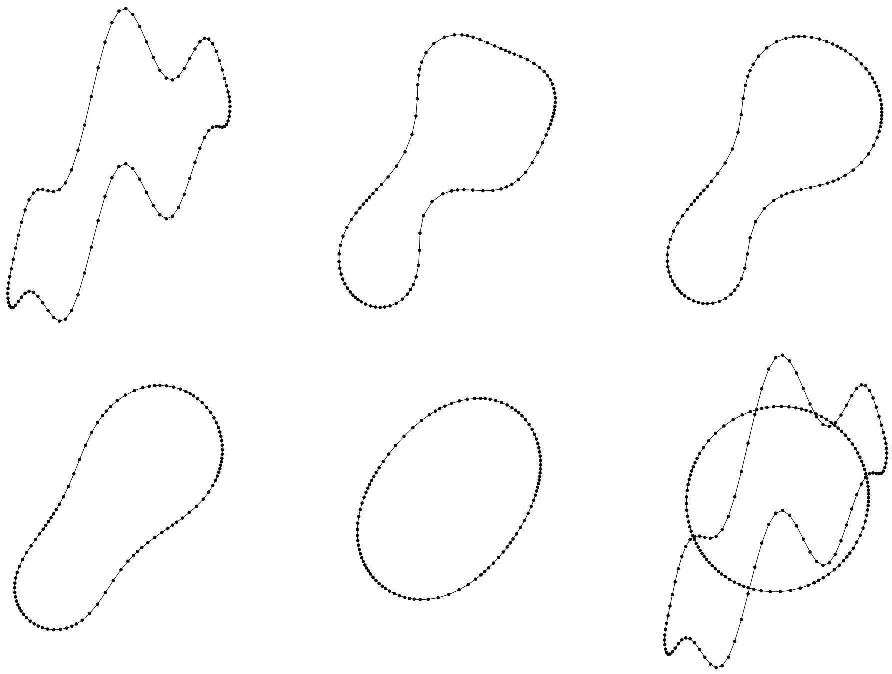

FIG. 5.2. *Evolution of the highly nonconvex curve plotted in time steps $t = 0, 0.002, 0.004, 0.015, 0.060$, and the last plot shows the initial curve and the asymptotical shape at time $t = 0.170$.*

Vision, 1 (1987), pp. 321–331.
[10] M. KIMURA, *Numerical analysis for moving boundary problems using the boundary tracking method,* Japan J. Indust. Appl. Math., 14 (1997), pp. 373–398.
[11] K. MIKULA, J. KAČUR, *Evolution of convex plane curves describing anisotropic motions of phase interfaces,* SIAM J. Sci. Comput., 17 (1996), pp. 1302–1327.
[12] K. MIKULA, *Solution of nonlinear curvature driven evolution of plane convex curves,* Applied Numerical Mathematics, 21 (1997), pp. 1–14.
[13] K. MIKULA, D. ŠEVČOVIČ, *Solution of nonlinearly curvature driven evolution of plane curves,* Applied Numerical Mathematics, 31 (1999), pp. 191–207.
[14] K. MIKULA, D. ŠEVČOVIČ, *Evolution of plane curves driven by a nonlinear function of curvature and anisotropy,* SIAM J. Appl. Math., 61 (2001), pp. 1473–1501.
[15] K. MIKULA, D. ŠEVČOVIČ, *Computational and qualitative aspects of evolution of curves driven by curvature and external force,* Comput. Visual. Sci., 6 (2004) pp. 211–225.
[16] G. SAPIRO, A. TANNENBAUM, *On affine plane curve evolution,* J. Funct. Anal., 119 (1994), pp. 79–120.

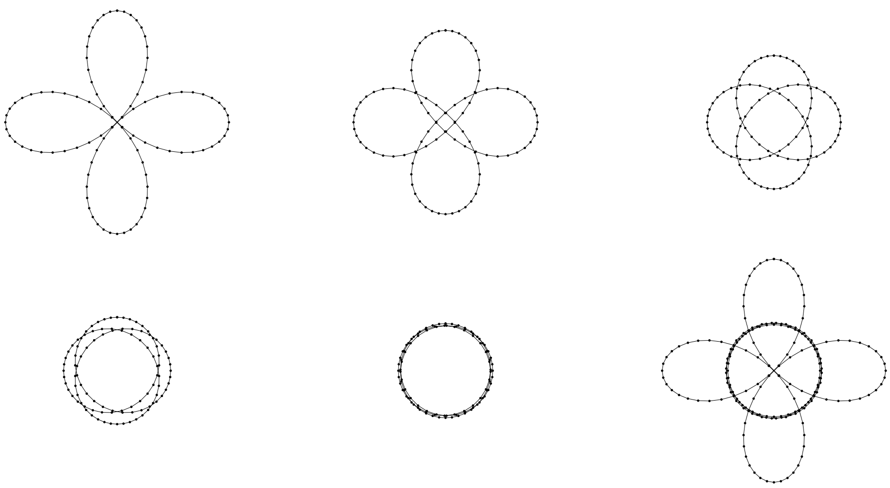

FIG. 5.3. *Evolution of the quatrefoil plotted in time steps* $t = 0, 0.01, 0.03, 0.05, 0.08$*, and the last plot shows the initial curve and the asymptotical shape at time* $t = 0.34$*. Since the index of quatrefoil curve is 3, it is asymptotically winding on 3-circle.*

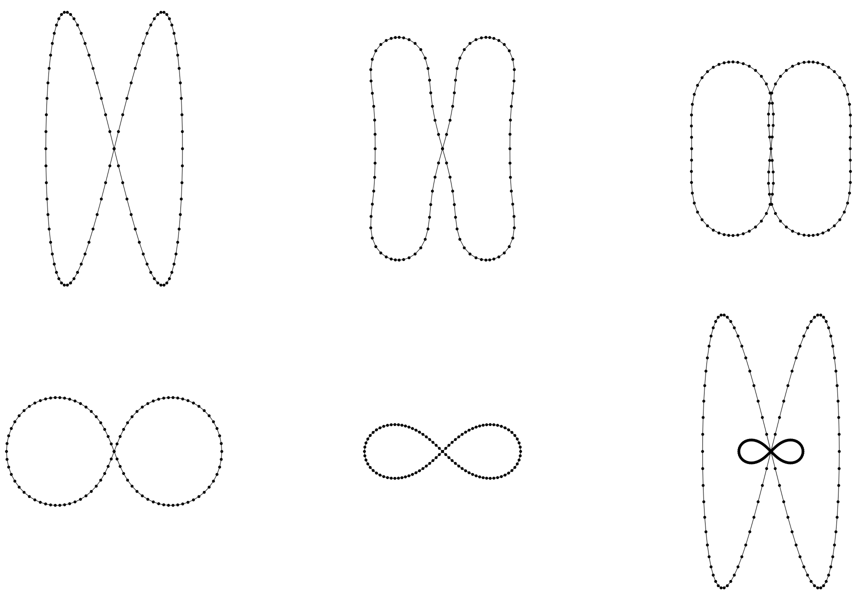

FIG. 5.4. *Evolution of the Lissajous curve plotted in time steps* $t = 0, 0.01, 0.06, 0.24, 0.60$*, and the last plot shows initial curve and the curve at time* $t = 0.66$ *just before shrinking. The Lissajous curve is shrinking to a point due to conservation of the zero enclosed area.*

[17] A. SARTI, G. CITTI, *A cortical based model of perceptual completion in the roto-translation space,* Preprint, University of Bologna, 2004.

[18] J.A. SETHIAN, *Level Set Methods and Fast Marching Methods: Evolving Interfaces in Computational Geometry, Fluid Mechanics, Computer Vision, and Material Science,* Cambridge University Press, New York, 1999.

[19] W. ZHU, T. CHAN, *Capture illusory comtours: a level set based approach,* CAM Report 03-65, UCLA, 2003.